Review

Non-routine Tracers for PET Imaging of High-grade Glioma

GUIDO FROSINA

Mutagenesis Unit, IRCCS AOU San Martino - IST, Genoa, Italy

Abstract. *Thorough imaging is crucial for diagnosis and treatment of high-grade gliomas (HGG), lethal brain tumours with median survival ranging 1-5 years after diagnosis. Positron-emission tomography (PET) is acquiring importance in imaging of HGG since it has the formidable advantage of providing information on tumour metabolism that may be critical for correct diagnosis and treatment planning. Recently employed PET tracers designed for the non-routine investigation of specific aspects of HGG metabolism, including hypoxia, neoangiogenesis, expression of integrins and stem cell markers, are reviewed herein. A thorough choice from among these non-routine tracers may provide important metabolic information complementing those obtained with more common PET analyses, for the sake of diagnostic, prognostic, treatment planning or research purposes.*

High-grade gliomas (HGG) are the most common malignant primary tumours of the central nervous system (CNS), representing a major cause of mortality in a young, productive subset of the population (1). HGG consist of glioblastomas (GB) [World Health Organization (WHO) grade IV], anaplastic astrocytomas (AA), anaplastic oligodendrogliomas (AO) and anaplastic oligoastrocytomas (WHO grade III) and some less common tumours such as anaplastic ependymomas and anaplastic gangliogliomas. Even with optimal treatment, median survival is 12-15 months for patients with GB and 2-5 years for those with anaplastic gliomas. The poor effectiveness of current treatments is linked to the infiltrative tumour nature, the presence of resistant tumour-driving cells (glioma-initiating cells, GIC) and the protective shield of the blood–brain (BBB) or blood–tumour barriers that restrict the passage of chemotherapeutics to the target tissues (2). Unlike therapy, diagnosis has much improved in recent years, with imaging playing an important role in evaluating the disease status of such patients (3). Computed tomography (CT) and magnetic resonance imaging (MRI) are first-line diagnostic procedures for HGG, with MRI showing higher resolution potency compared to CT, by allowing the dynamic acquisition of images after injection of intravenous contrast (CE-MRI) or providing information on cellular density by diffusion-weighted MRI and angiogenesis by perfusion-weighted MRI.

With the continuous emergence of new classes of tracers, PET may specifically characterize major metabolic processes in brain tumours such as carbohydrate and amino-acid metabolism, DNA synthesis and many others which help in diagnosis, prognosis and assessment of experimental therapies. Consistently, micro-PET devices developed for pre-clinical research hold increasing roles in animal studies of HGG. Several excellent reviews on the most common tracers for PET of HGG, including of ^{11}C-L-methionine (^{11}C-MET), ^{18}F-2-fluoro-2-deoxy-D-glucose (^{18}F-FDG), ^{18}F-3,4-dihydroxy-6-fluoro-l-phenylalanine (^{18}F-FDOPA) and ^{18}F-O-(2-fluoroethyl)-L-tyrosine (^{18}F-FET) have been recently published (2,4-7). Herein, we discuss non-routine classes of radiotracers recently employed for investigation of specific metabolic aspects of HGG. Articles were searched in PubMed using the general terms “PET and glioma” for the publication year 2014 (either in print or Epub ahead of print) and further selected for their specific use (Table I).

Tracers Using ^{11}C

^{11}CMethylAMD3465. The C-X-C chemokine receptor type 4 (CXCR4) plays a role during progression of some tumours including HGG (8). The PET imaging of the radiolabeled selective CXCR4 receptor antagonist ^{11}Cmethyl-AMD3465 has been studied in rats bearing C6 HGG xenografts. PET demonstrated specific accumulation of the tracer in the

Correspondence to: Dr. Guido Frosina, Mutagenesis Unit, IRCCS Azienda Ospedaliera Universitaria San Martino - IST Istituto Nazionale per la Ricerca sul Cancro, 16132 Genova, Italy. Tel: +39 0105558543, Fax: +39 0105558237, e-mail: guido.frosina@hsanmartino.it

Key Words: Diagnostic techniques and procedures; functional neuroimaging; glioblastoma; glioma; radionuclide imaging, review.

Table I. *Non-routine, recently employed positron-emission tomography (PET) tracers for high-grade glioma as reported by articles in 2014.*

Tracer atom	Half-life (min) (keV)	Decay by positron emission	Max energy study	Molecule application	Type of results	Main	Main features/	Ref
^{11}C	20.3	99.8%	960	Methyl-AMD3465	Preclinical	Diagnosis	Detects CXCR4 expression	(8)
				(R)PK11195	Clinical	Diagnosis therapy	TSPO ligand	(9)
				DMCYS	Preclinical	Diagnosis	Better than the corresponding L-isomers as tumour-detecting agent or than MET in the differentiation of tumour from inflammation	(10)
^{62}Cu	9.7	98%	2925	ATSM	Clinical	Diagnosis	Information to differentiate GB from other brain neoplasms and to identify hypoxic regions	(11)
^{64}Cu	762.0	19%	657	NOTA-AC133 MAB	Preclinical	Diagnosis	Detection of AC133^{+} tumour stem cells in subcutaneous and orthotopic glioma xenografts	(13)
				DOTA-TNYL-RAW peptide	Preclinical	Diagnosis	Molecular imaging agent for PET/CT of GB owing to its ability to bind to both EphB4-expressing angiogenic blood vessels and EphB4-expressing tumour cells	(14)
^{18}F	109.7	97%	633	F-14	Preclinical	Diagnosis	TSPO ligand	(15)
				FACBC	Preclinical	Diagnosis	Low FACBC uptake in granulocytes/ macrophages may be advantageous in discriminating inflamed regions from tumours	(16)
				FBuEA-GS	Preclinical	Diagnosis	L-PGDS ligand	(17)
				FPIA	Preclinical	Diagnosis	Contributes to detect aberrant lipid metabolism	(18)
				FRP170	Clinical	Diagnosis	Accumulation on ^{18}F-FRP170 PET may represent hypoxic tissues	(19)
				NaF	Clinical	Diagnosis	May allow detection of osseous metastases	(20)
				VUIIS1008	Preclinical	Diagnosis	TSPO ligand	(21)
^{68}Ga	67.7	89%	1920	A2B1	Preclinical	Diagnosis	Allows imaging of tumour-associated $\alpha 2\beta 1$ integrin expression with special sensitivity after FUS treatment (sonoporation)	(22)
				DOTATOC	Preclinical Clinical	Diagnosis Therapy	Somatostatin analog binding to SSTR2 but gives low tumour signals *in vivo* Used in RGS studies as a surrogate of ^{90}Y-labelled molecule	(23, 24)
				DOTA-Z09591	Preclinical	Diagnosis	Imaging of PDGFRβ, a transmembrane tyrosine kinase receptor involved in angiogenesis	(25)
				PRGD2	Clinical	Diagnosis RT planning	Allows glioma demarcation more thoroughly than ^{18}F-FDG. Superior to ^{18}F-FDG in differentiating HGG from LGG by different accumulation patterns in the two grades	(27)
^{124}I	6019.2	23.0%	2138	8H9	Preclinical	Therapy Diagnosis	^{124}I conjugated to the antiglioma monoclonal antibody 8H9 may serve as a 'theragnostic' agent delivered *via* CED to DIPG	(30)
^{13}N	9.97	99.8%	1200.3	NH3	Clinical	Diagnosis	Combination with ^{18}F-FDG PET/CT demonstrates that perfusion and metabolism are coupled in recurrent HGG, indicating that the two tracers target two different but interrelated aspects	(31)

tumour and other CXCR4-expressing organs, such as lymph node, liver, bone marrow and spleen, and elevated tumour-to-muscle and tumour-to-plasma ratios were found, suggesting that ^{11}C-methyl-AMD3465 may detect physiological CXCR4 expression in HGG (8).

^{11}C-(R)PK11195. Elevated expression of the 18-kDa mitochondrial translocator protein (TSPO) may correlate with disease progression and aggressive, invasive behaviour of a variety of solid tumours, including HGG, while being rare in normal tissues. TSPO can be imaged by PET using the selective radiotracer ^{11}C-(R)PK11195. The binding potential of ^{11}C-(R)PK11195 in HGG has been found to be significantly higher than in low-grade gliomas (LGG) in a clinical study (9) (Figure 1A). TSPO in gliomas was

expressed predominantly by neoplastic cells and its expression correlated positively with binding potential of ^{11}C-(R)PK11195 in the tumours. Hence, PET with ^{11}C-(R)PK11195 in HGG may predominantly reflect TSPO expression, and patient candidates for TSPO-targeting therapies may by stratified by this procedure.

**11C-Methyl-D-cysteine ("c-DMCYS)*. The D-amino acid isomer of *11C-methyl-cysteine has been proposed as a PET tracer potentially useful for discriminating tumour from inflamed tissues in animal models. PET imaging of orthotopic HGG models with ^{11}C-methyl-D-cysteine have further shown a fair tumour to normal brain tissue (T/N) ratio (10).

Tracers Using ^{62}CU and ^{64}CU

^{62}CU-diacetyl-bis (N4-methylthiosemicarbazone) (^{62}CU-ATSM). Tumour hypoxia assessed by ^{62}CU-ATSM PET/CT correlates with diffusion capacity obtained by diffusion-weighted imaging and may be useful for grading gliomas (11). Maximum standardized uptake (SUV) and T/N values of ^{62}CU-ATSM were significantly higher in human GB than in normal or lower grade tumour tissues, while limited differences were observed in parallel studies from the same group with ^{18}F-FDG (12). ^{62}CU-ATSM PET/CT may also provide diagnostic information to differentiate GB from other brain neoplasms such as CNS lymphomas (11).

^{64}Cu-1,4,7-Triazacyclononane-1,4,7-triacetic acid (NOTA)-AC133 monoclonal antibody (^{64}Cu-NOTA-AC133 MAB). The AC133 epitope of CD133 is a widely used tumour stem cell marker for intra- and extracranial tumours. The non-invasive detection of AC133-overexpressing tumour cells by PET in subcutaneous and orthotopic glioma xenografts using antibody-based tracers has been described (Figure 1B) (13). Micro-PET with ^{64}Cu-NOTA-AC133 MAB yielded images with elevated T/N contrast, delineating subcutaneous tumour stem cell-derived xenografts. Intracerebral tumours as small as 2-3 mm were also discernible and the micro-PET images reflected the invasive growth pattern of orthotopic GIC-derived tumours with physiological density of AC133$^+$ cells (13).

^{64}Cu-1,4,7,10-Tetra-azocyclododecane-N,N'N'',N'''-tetra-acetic acid (DOTA)-TNYL-RAW peptide. The ephrin type-B receptor 4 (EPHB4) receptor, a member of the tyrosine kinase receptor family, may be overexpressed in both tumour cells and angiogenic blood vessels of HGG and the EPHB4-binding peptide TNYL-RAW labelled with ^{64}Cu has been examined as a PET tracer for orthotopic human HGG (14). TNYL-RAW was conjugated to the radiometal chelator DOTA and the conjugate was then labelled with ^{64}Cu for *in vivo* dual micro-PET/CT in nude mice orthotopically implanted with EPHB4-expressing U251 and EPHB4-negative U87 human GB cells. In U251 tumours, the labelled peptide co-localized with both tumour blood vessels and tumour cells; in U87 tumours, the tracer co-localized with tumour blood vessels only, not with tumour cells, indicating that the labelled EPHB4-specific peptide might be a possible tool for imaging both GB growth and neo-angiogenesis (14). A specific problem associated with ^{64}Cu-labelled polypeptides relates to the instability of the copper chelates and efforts are being made to develop new bi-functional chelating agents for preparing more stable ^{64}Cu-labelled polypeptides.

Tracers Using ^{18}F

^{18}F-7-Chloro-N,N,5-trimethyl-4-oxo-3(6-fluoropyridin-2-yl)-3,5-dihydro-4H-pyridazino[4,5-b]indole-1-acetamide (^{18}F-14). As aforementioned [see ^{11}C-(R)PK11195] the 18-kDa mitochondrial TSPO is up-regulated in HGG (9) (Figure 1A). Focused structure–activity relationship studies have recently led to the development of a further fluorinated TSPO ligand with specific affinity identified by the number "14". "14" was radiolabeled with fluorine-18 (^{18}F-14) in fair yield and specific activity and *in vivo* studies on ^{18}F-14 as a probe for molecular imaging of TSPO-expressing HGG tumours are ongoing (15). One additional TSPO ^{18}F-ligand developed for HGG PET will be discussed later (^{18}F-VUIIS1008).

^{18}F-Trans-1-amino-3-fluorocyclobutanecarboxylic acid (^{18}F-FACBC). This is a synthetic amino acid analog for PET that is currently being tested in phase II clinical trials for prostate cancer (http://aojnmb.mums.ac.ir/article_2842_398.html). The mechanisms of uptake of ^{18}F-FACBC in C6 glioma rat cells and inflammatory cells have been investigated in comparison to those of ^{18}F-FDG (16). Over half of ^{18}F-FACBC uptake by glioma C6 cells was mediated by Na^+-dependent amino acid transporters and ^{18}F-FACBC uptake ratios of granulocytes/macrophages to tumour cells were lower than those for ^{18}F-FDG, indicating that PET with ^{18}F-FACBC might be advantageous in discriminating inflamed regions from tumours (16).

^{18}F-Fluorobutyl ethacrynic amide (^{18}F-FBuEA-GS). Lipocalin-type prostaglandin D synthase (L-PGDS) expression has been correlated with the progression of neurological disorders including some brain tumours. The imaging potency of a glutathione (GS) conjugate of the L-PGDS ligand, ^{18}F-FBuEA-GS, for HGG was investigated in a rat model (17). ^{18}F-FBuEA-GS was found to bind specifically to L-PGDS and the PET imaging suggested that the radiotracer accumulation in tumour lesions was mediated by the GS moiety and related to the overexpression of L-PGDS (17).

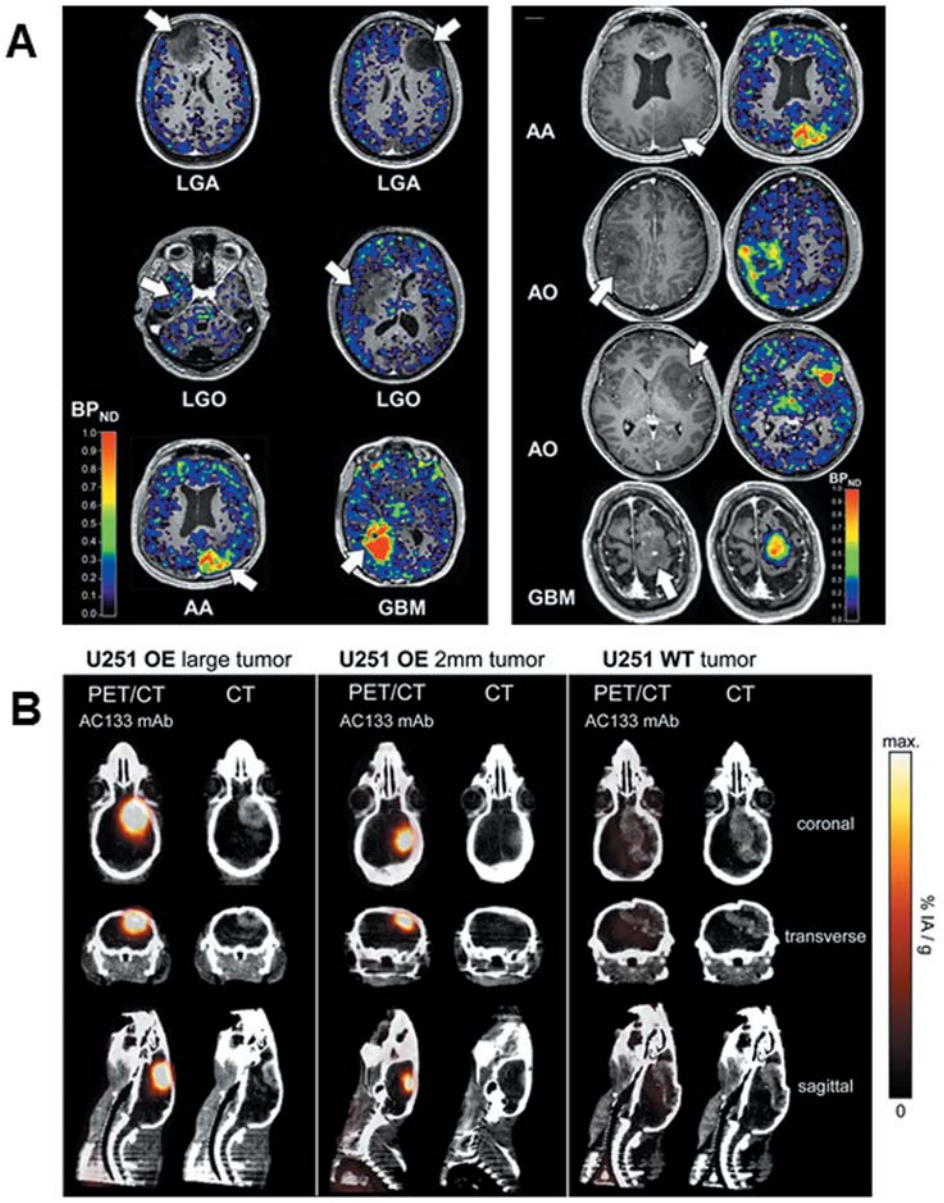

Figure 1. *Clinical and preclinical studies with recently employed, non-routine positron-emission tomography (PET) tracers. A: Left: Co-registered and fused postcontrast T1-weighted magnetic resonance (MR) images (gray-scale) and parametric binding potential (BP_{ND}) images (colour spectrum) of representative cases of low-grade astrocytoma (LGA), low-grade oligodendroglioma (LGO) and glioblastoma (GBM). BP_{ND} is low in LGA, whereas foci with high BP_{ND} are found in LGO and areas of high BP_{ND} in GBM (arrows). Right: Co-registered postcontrast T1-weighted MR images and parametric BP_{ND} images in four HGGs showing little or no contrast enhancement (arrows) and high ^{11}C-(R)PK11195 binding within tumours. Colour bars denote BP_{ND} values. From (9) with permission. B: PET/computed tomographic (CT) imaging and biodistribution of ^{64}Cu-NOTA-AC133 MAB in mice bearing orthotopic U251 glioma xenografts. Nude mice bearing orthotopic xenografts of U251 glioma cells overexpressing CD133 or orthotopic xenografts of CD133−negative U251 wild-type cells received 7.5±0.8 MBq ^{64}Cu-NOTA-AC133 MAB via tail vein injection and PET/CT images were acquired 24 and 48 h later. Representative contrast-enhanced micro-CT and fused micro-PET/CT sections from mice bearing CD133-overexpressing U251 gliomas (left, centre) and from mice bearing U251 wild-type tumours (right) are shown. For the PET/CT images, an upper threshold corresponding to the maximum tracer uptake of the CD133-overexpressing U251 tumours was chosen. From (13) with permission.*

^{18}F-Fluoro-pivalic acid (^{18}F-FPIA). In addition to increased glycolytic flux, tumour cells may display aberrant lipid metabolism. Pivalic acid is a short-chain, branched carboxylic acid used to increase oral bioavailability of prodrugs. After prodrug hydrolysis, pivalic acid undergoes intracellular metabolism *via* the fatty acid oxidation pathway.

The new fluorinated probe ^{18}F-FPIA was designed for the imaging of aberrant lipid metabolism in HGG tissues (18). Compared with ^{18}F-FDG in an animal model of U87 tumour, ^{18}F-FPIA had lower normal-brain uptake resulting in a superior T/N ratio and higher contrast for brain cancer imaging. Both radiotracers showed yet significant unspecific localization in inflammatory tissues (18).

^{18}F-1-(2-Fluoro-1-[hydroxymethyl]ethoxy)methyl-2-nitroimidazole (^{18}F-FRP170). This compound has been described as a further hypoxic cell tracer for GB (19). Patients underwent PET with ^{18}F-FRP170 before tumour resection and the mean SUV was calculated at tumour regions showing high or low accumulation of ^{18}F-FRP170. In those areas, intratumoural pO_2 was also measured using microelectrodes during tumour resection. The mean pO_2 was significantly lower in the areas of high uptake than in those of low uptake, suggesting that high accumulation of ^{18}F-FRP170 might indicate viable hypoxic tissues in GB.

^{18}F-Sodium fluoride (^{18}F-NaF). One rare case of osseous metastases from GB diagnosed by ^{18}F-NaF PET/CT has been reported (20). A 30-year-old man with a history of GB presented with bone pain and underwent ^{18}F-NaF PET/CT for further evaluation. Intense uptake in two bone lesions was noted and histopathological evaluation revealed osseous metastases from GB. Hence, albeit rare, bone metastases have to be considered in patients with axial tumours and atraumatic bone pain and ^{18}F-NaF PET/CT may be taken into consideration for their detection (20).

^{18}F-2-(5,7-Diethyl-2-(4-(2-fluoroethoxy)phenyl)pyrazolo[1,5-a]pyrimidin-3-yl)-N,N-diethylacetamide (^{18}F-VUIIS1008). Besides the aforementioned ^{11}C-(R)PK11195 and ^{18}F-14, one further high-affinity TSPO PET ligand, ^{18}F-VUIIS1008, has been evaluated in healthy mice and HGG-bearing rats. Dynamic PET data were acquired after ^{18}F-VUIIS1008 injection, with binding reversibility and specificity evaluated by non-radioactive ligand displacement or blocking. Imaging was validated by histology and immunohistochemistry. ^{18}FVUIIS1008 exhibited rapid uptake in TSPO-rich organs, as well as elevated T/N and binding potential in tumour tissues. Blocking of uptake and binding could be obtained by competing treatment with non-radioactive VUIIS1008 (21).

Tracers Using ^{68}GA

^{68}Ga-NOTA-15-amino-4,7,10,13-tetraoxapentadecanoic acid (PEG4)-cyclo (GDGEAyK) (^{68}Ga-A2B1). Integrin α2β1 may be highly expressed in HGG and is currently being explored as a prognostic biomarker for these tumours. A novel ^{68}Ga-labeled integrin α2β1-targeted PET tracer ^{68}Ga-A2B1 was designed and evaluated in preclinical models of GB. ^{68}Ga-A2B1 PET was performed in subcutaneous U87 tumour-bearing athymic mice and receptor targeting specificity was confirmed by competition blocking. However, due to quick renal washout and lability of peptide tracers in the blood stream, the focused ultrasound-mediated delivery method was adopted to enhance tumour uptake and retention of tracers. The average radioactivity accumulation within a tumour was quantified from the multiple region of interest volumes and was analysed in accordance with the *ex vivo* autoradiographic and pathological data. A significant increase in tumour uptake of ^{68}Ga-A2B1 was observed following focused ultrasound treatment, indicating a possible (although difficult to be clinically applied) enhancement procedure for PET imaging of HGG (22).

^{68}Ga-DOTA-tyr3-octreotide (^{68}GaDOTATOC). Somatostatin receptor subtype 2 (SSTR2) has been proposed as a potential target in HGG and its visualization and quantification could be useful for development of SSTR2-targeted therapies. Rat BT4C malignant glioma cells were injected into rat brain or subcutaneously into nude mice in order to investigate the tumour uptake of ^{68}GaDOTATOC, a somatostatin analogue binding to SSTR2 (23). Albeit high T/N and tumour-to-muscle ratios of ^{68}Ga-DOTATOC were observed by autoradiography, tumour signals detected *in vivo* were too low, thus compromising PET imaging and confirming the indispensability of animal investigations in this kind of studies (23). DOTATOC has been also explored in radioguided surgery (RGS) of HGG. This technique is based on selective delivery of beta$^-$ radiation to the tumour by a tumour-specific emitting molecule. A study of the uptake of the beta$^-$-emitting molecule ^{90}Y-DOTATOC and a feasibility study of the RGS technique in HGG patients have been reported (24). Uptake and background were estimated using the surrogate molecule ^{68}Ga-DOTATOC assuming that gallium and yttrium are chemically similar enough for the kinetics of the tracer not to differ. The T/N of ^{68}Ga-DOTATOC in HGG was more than 4, implying that the tracer might be selective enough for RGS (24).

^{68}Ga-DOTA-conjugated Z0959 affibody (^{68}Ga-DOTA-Z09591). Overexpression and oversignalling of the angiogenesis biomarker/tyrosine kinase receptor platelet-derived growth factor receptor beta (PDGFRβ) has been observed in multiple malignant tumours including HGG (25). Recently, the affibody molecule Z09591 labelled with ^{111}In has been demonstrated to be able to specifically target PDGFRβ-expressing tumours for *in vivo* imaging. ^{68}Ga-DOTA-Z09591 has shown the capacity to specifically bind to PDGFRβ-expressing U87 GB cells *in vitro* (26). *In vivo*, ^{68}Ga-DOTA-Z09591 demonstrated specific targeting of U87 GB xenografts in immunodeficient mice with a remarkable

tumour-to-blood activity ratio of 8.0. Micro-PET imaging consistently provided high-contrast imaging of U87 GB xenografts (25).

^{68}Ga-S-2-(4-Isothiocyanatobenzyl)-1,4,7-triazacyclononane-1,4,7-triacetic acid-PRGD2 (^{68}Ga-PRGD2). The integrin αvβ3 is overexpressed in both neovasculature and glioma cells. ^{68}Ga-PRGD2 has been described as a new agent for non-invasive imaging of αvβ3 in patients with HGG (27). ^{68}Ga-PRGD2 specifically accumulated in brain tumours that were rich in αvβ3 and other neovasculature markers, but not in brain parenchyma other than the choroid plexus. ^{68}Ga-PRGD2 PET/CT demarcated the tumour more specifically than ^{18}F-FDG PET/CT and the maximum SUV of ^{68}Ga-PRGD2 correlated with the glioma grading (27).

Tracers Using ^{124}I

^{124}I-8H9 monoclonal antibody. Convection enhanced delivery (CED) is a promising, albeit tricky drug delivery mode for treating brain tumours (28,29). Thorough measurement of the volume of distribution (V_D) of CED-infused agents in the human brain is crucial for successful treatment. ^{124}I may be a suitable radionuclide for *in vivo* measurement of volume of distribution *via* PET and due to the potential utility of radioimmunotherapy, ^{124}I-8H9 delivered *via* CED has been evaluated as a 'theragnostic' agent against pediatric tumour diffuse intrinsic pontine glioma (DIPG). In preclinical dosimetric studies, rats were subjected to CED of ^{124}I-8H9 to the pons with serial micro-PET performed during the subsequent 7 days. Two primates were also subjected to CED of ^{124}I-8H9 to the pons for safety and dosimetric analyses. The mean V_D was 0.14 cc^3 in the rat and 6.2 cc^3 in the primates (30) and the activity decreased 10-fold 48 h after CED in both animal models. Further studies on CED of ^{124}I-8H9 for DIPG might be warranted.

Tracers Using ^{13}N

^{13}N-Ammonia (^{13}N-NH_3). A perfusion–metabolism-coupled analytical procedure with ^{13}N-NH_3 and ^{18}F-FDG PET/CT has been reported in recurrent GB (31). ^{13}N-NH_3 PET/CT and ^{18}F-FDG PET/CT have been found concordant in essentially all investigated patients. Overall sensitivity, specificity, predictive values and accuracy were >75% for both ^{13}N-NH_3 PET/CT and ^{18}F-FDG PET/CT. The performance of ^{13}N-NH_3 PET/CT and ^{18}F-FDG PET/CT were not significantly different between HGG and LGG and a positive correlation was noted between the SUV derived in the two modalities. It has thus been proposed that perfusion analysed with ^{13}N-NH_3 and metabolism analysed with ^{18}F-FDG may be coupled in HGG analysis, targeting two different but interrelated aspects of the same pathological process (31).

Prospects for Non-routine PET in Imaging of HGG

A number of issues must be considered when PET is used for imaging HGG: the variety of PET machines and tracers, the heterogeneity of the protocols used for image acquisition and the existence of semi-quiescent but highly invasive GIC (32). Specific concerns for preclinical studies of micro-PET relate to the frequent use of orthotopic tumour animal models developed by intracranial injection of established, non-GIC lines. The poor infiltrating and neovasculariing capacities of orthotopic tumours developed by established cell lines such as U87 may possibly bias radiotracer biodistribution and uptake in micro-PET studies (33). Dealing with these issues may include the harmonisation of protocols and software applications as well as the use of primary GIC lines that more closely mimic clinical tumour features (33). That said, following thorough radiopharmaceutical development, PET with specific tracers may provide important information on tumour metabolism and response to therapies as well as for determining the pharmacokinetics of novel drugs. Merely to quote one pair of examples, the pharmacokinetics of ataxia telangiectasia mutated inhibitors (ATMi) that are capable of specifically radiosensitizing GIC-driven tumours (34) or peptides inhibiting the myelocytomatosis (MYC) oncoprotein (MYCi Omomyc peptides) (35) that are promising targeting chemotherapeutics, could be conveniently studied by PET. After rational drug design by *in silico* modelling, labelling the basic ATMi KU60019 molecule or the basic MYCi Omomyc peptide with appropriate radionuclides (*e.g.* ^{18}F) will allow investigation of the biodistribution and pharmacokinetics of these novel therapeutic agents by static and dynamic PET in the preclinical and then clinical settings (28, 34-37).

Conflicts of Interest

The Author declares that he has no conflict of interest in regard to this article.

Acknowledgements

This work was partially supported by Compagnia San Paolo, Turin, Italy (grant no. 2010.1944 and the project "Terapie innovative per il glioblastoma").

References

1 Ahmed R, Oborski MJ, Hwang M, Lieberman FS and Mountz JM: Malignant gliomas: current perspectives in diagnosis, treatment, and early response assessment using advanced quantitative imaging methods. Cancer Manag Res *6*: 149-170, 2014.

2 Heiss WD: PET in gliomas. Overview of current studies. Nuklearmedizin *53*: 163-171, 2014.

3 Frosina G: Limited advances in therapy of glioblastoma trigger re-consideration of research policy. Crit Rev Oncol *96(2)*: 257-261, 2015.

4 Heiss WD: Clinical impact of amino acid PET in gliomas. J Nucl Med *55*: 1219-1220, 2014.

5 Suchorska B, Tonn JC and Jansen NL: PET imaging for brain tumor diagnostics. Curr Opin Neurol *27*: 683-688, 2014.

6 Galldiks N and Langen KJ: Applications of PET imaging of neurological tumors with radiolabeled amino acids. Q J Nucl Med Mol Imaging *59*: 70-82, 2015.

7 Galldiks N, Langen KJ and Pope WB: From the clinician's point of view – What is the status quo of positron-emission tomography in patients with brain tumors? Neuro Oncol 17: 1434-1444, 2015.

8 Hartimath SV, van Waarde A, Dierckx RA and de Vries EF: Evaluation of N-[C]Methyl-AMD3465 as a PET tracer for imaging of CXCR4 receptor expression in a C6 glioma tumor model. Mol Pharm *11(11)*: 3810-3817, 2014.

9 Su Z, Roncaroli F, Durrenberger PF, Coope DJ, Karabatsou K, Hinz R, Thompson G, Turkheimer FE, Janczar K, Du Plessis D, Brodbelt A, Jackson A, Gerhard A and Herholz K: The 18-kDa mitochondrial translocator protein in human gliomas: an ^{11}C-(R)PK11195 PET imaging and neuropathology study. J Nucl Med *56*: 512-517, 2015.

10 Huang T, Tang G, Wang H, Nie D, Tang X, Liang X, Hu K, Yi C, Yao B and Tang C: Synthesis and preliminary biological evaluation of S-(11)C-methyl-D-cysteine as a new amino acid PET tracer for cancer imaging. Amino Acids *47*: 719-727, 2015.

11 Hino-Shishikura A, Tateishi U, Shibata H, Yoneyama T, Nishii T, Torii I, Tateishi K, Ohtake M, Kawahara N and Inoue T: Tumor hypoxia and microscopic diffusion capacity in brain tumors: a comparison of (62)Cu-diacetyl-*bis* (*N*4-methylthiosemicarba-zone) PET/CT and diffusion-weighted MR imaging. Eur J Nucl Med Mol Imaging *41*: 1419-1427, 2014.

12 Tateishi K, Tateishi U, Nakanowatari S, Ohtake M, Minamimoto R, Suenaga J, Murata H, Kubota K, Inoue T and Kawahara N: (62)Cu-diacetyl-*bis* (*N*(4)-methylthiosemicarbazone) PET in human gliomas: comparative study with [(18)F]fluoro-deoxyglucose and L-methyl-[(11)C]methionine PET. AJNR Am J Neuroradiol *35*: 278-284, 2014.

13 Gaedicke S, Braun F, Prasad S, Machein M, Firat E, Hettich M, Gudihal R, Zhu X, Klingner K, Schuler J, Herold-Mende CC, Grosu AL, Behe M, Weber W, Macke H and Niedermann G: Noninvasive positron-emission tomography and fluorescence imaging of CD133+ tumor stem cells. Proc Natl Acad Sci USA *111*: E692-701, 2014.

14 Huang M, Xiong C, Lu W, Zhang R, Zhou M, Huang Q, Weinberg J and Li C: Dual-modality micro-positron emission tomography/computed tomography and near-infrared fluorescence imaging of EphB4 in orthotopic glioblastoma xenograft models. Mol Imaging Biol *16*: 74-84, 2014.

15 Cheung YY, Nickels ML, Tang D, Buck JR and Manning HC: Facile synthesis of SSR180575 and discovery of 7-chloro-*N,N*,5-trimethyl-4-oxo-3(6-[(18)F]fluoropyridin-2-yl)-3,5-dihydro-4H-pyri dazino[4,5-b]indole-1-acetamide, a potent pyridazinoindole ligand for PET imaging of TSPO in cancer. Bioorg Med Chem Lett *24*: 4466-4471, 2014.

16 Oka S, Okudaira H, Ono M, Schuster DM, Goodman MM, Kawai K and Shirakami Y: Differences in transport mechanisms of trans-1-amino-3-[^{18}F]fluorocyclobutanecarboxylic acid in inflammation, prostate cancer, and glioma cells: comparison with L-[methyl-11C]methionine and 2-deoxy-2-[^{18}F]fluoro-D-glucose. Mol Imaging Biol *16*: 322-329, 2014.

17 Huang HL, Huang YC, Lee WY, Yeh CN, Lin KJ and Yu CS: ^{18}F-Glutathione conjugate as a PET tracer for imaging tumors that overexpress L-PGDS enzyme. PLoS One 9: e104118, 2014.

18 Witney TH, Pisaneschi F, Alam IS, Trousil S, Kaliszczak M, Twyman F, Brickute D, Nguyen QD, Schug Z, Gottlieb E and Aboagye EO: Preclinical evaluation of 3-18F-fluoro-2,2-dimethylpropionic acid as an imaging agent for tumor detection. J Nucl Med *55*: 1506-1512, 2014.

19 Beppu T, Terasaki K, Sasaki T, Fujiwara S, Matsuura H, Ogasawara K, Sera K, Yamada N, Uesugi N, Sugai T, Kudo K, Sasaki M, Ehara S, Iwata R and Takai Y: Standardized uptake value in high uptake area on positron emission tomography with ^{18}F-FRP170 as a hypoxic cell tracer correlates with intratumoral oxygen pressure in glioblastoma. Mol Imaging Biol *16*: 127-135, 2014.

20 Derlin T, Clauditz TS and Bannas P: Glioblastoma multiforme metastastic to the bone: diagnosis by (18)F-NaF PET/CT. Clin Nucl Med *39*: 188-189, 2014.

21 Tang D, Nickels ML, Tantawy MN, Buck JR and Manning HC: Preclinical imaging evaluation of novel TSPO-PET ligand 2-(5,7-diethyl-2-(4-(2-[F]fluoroethoxy)phenyl)pyrazolo[1,5-a]pyrimidin-3-yl)-*N,N*-diethylacetamide ([^{18}F]VUIIS1008) in Glioma. Mol Imaging Biol *16(6)*: 813-820, 2014.

22 Chung YH, Hsu PH, Huang CW, Hsieh WC, Huang FT, Chang WC, Chiu H, Hsu ST and Yen TC: Evaluation of prognostic integrin alpha2beta1 PET tracer and concurrent targeting delivery using focused ultrasound for brain glioma detection. Mol Pharm *11(11)*: 3904-3914, 2014.

23 Kiviniemi A, Gardberg M, Autio A, Li XG, Heuser VD, Liljenback H, Kakela M, Sipila H, Kurkipuro J, Yla-Herttuala S, Knuuti J, Minn H and Roivainen A: Feasibility of experimental BT4C glioma models for somatostatin receptor 2-targeted therapies. Acta Oncol *53*: 1125-1134, 2014.

24 Collamati F, Pepe A, Bellini F, Bocci V, Chiodi G, Cremonesi M, De Lucia E, Ferrari ME, Frallicciardi PM, Grana CM, Marafini M, Mattei I, Morganti S, Patera V, Piersanti L, Recchia L, Russomando A, Sarti A, Sciubba A, Senzacqua M, Solfaroli Camillocci E, Voena C, Pinci D and Faccini R: Toward radioguided surgery with beta- decays: uptake of a somatostatin analogue, DOTATOC, in meningioma and high-grade glioma. J Nucl Med *56*: 3-8, 2015.

25 Strand J, Varasteh Z, Eriksson O, Abrahmsen L, Orlova A and Tolmachev V: Gallium-68-labeled affibody molecule for PET imaging of PDGFRbeta expression *in vivo*. Mol Pharm *11(11)*: 3957-3964, 2014.

26 Tolmachev V, Varasteh Z, Honarvar H, Hosseinimehr SJ, Eriksson O, Jonasson P, Frejd FY, Abrahmsen L and Orlova A: Imaging of platelet-derived growth factor receptor beta expression in glioblastoma xenografts using affibody molecule ^{111}In-DOTA-Z09591. J Nucl Med *55*: 294-300, 2014.

27 Li D, Zhao X, Zhang L, Li F, Ji N, Gao Z, Wang J, Kang P, Liu Z, Shi J, Chen X and Zhu Z: Ga-PRGD2 PET/CT in the Evaluation of Glioma: A Prospective Study. Mol Pharm *11(11)*: 3923-3929, 2014.

28 Frosina G: The glioblastoma problem: targeting by combined medicinal chemistry approaches. Curr Med Chem *22*: 2506-2524, 2015.

29 Ung TH, Malone H, Canoll P and Bruce JN: Convection-enhanced delivery for glioblastoma: targeted delivery of antitumor therapeutics. CNS Oncol *4(4)*: 225-234:1-10, 2015.

30 Luther N, Zhou Z, Zanzonico P, Cheung NK, Humm J, Edgar MA and Souweidane MM: The potential of theragnostic ^{124}I-8H9 convection-enhanced delivery in diffuse intrinsic pontine glioma. Neuro Oncol *16(6)*: 800-806, 2014.

31 Khangembam BC, Karunanithi S, Sharma P, Kc SS, Kumar R, Julka PK, Kumar R and Bal C: Perfusion-metabolism coupling in recurrent gliomas: a prospective validation study with N-ammonia and F-fluorodeoxyglucose PET/CT. Neuroradiology *56(10)*: 893-902, 2014.

32 Dhermain F: Radiotherapy of high-grade gliomas: current standards and new concepts, innovations in imaging and radiotherapy, and new therapeutic approaches. Chin J Cancer *33*: 16-24, 2014.

33 Frosina G: Development of therapeutics for high-grade gliomas using orthotopic rodent models. Curr Med Chem *20*: 3272-3299, 2013.

34 Vecchio D, Daga A, Carra E, Marubbi D, Raso A, Mascelli S, Nozza P, Garre ML, Pitto F, Ravetti JL, Vagge S, Corvo R, Profumo A, Baio G, Marcello D and Frosina G: Pharmacokinetics, pharmacodynamics and efficacy on pediatric tumors of the glioma radiosensitizer KU60019. Int J Cancer *136*: 1445-1457, 2015.

35 Annibali D, Whitfield JR, Favuzzi E, Jauset T, Serrano E, Cuartas I, Redondo-Campos S, Folch G, Gonzalez-Junca A, Sodir NM, Masso-Valles D, Beaulieu ME, Swigart LB, Mc Gee MM, Somma MP, Nasi S, Seoane J, Evan GI and Soucek L: Myc inhibition is effective against glioma and reveals a role for Myc in proficient mitosis. Nat Commun *5*: 4632, 2014.

36 Vecchio D, Daga A, Carra E, Marubbi D, Baio G, Neumaier CE, Vagge S, Corvo R, Pia Brisigotti M, Louis Ravetti J, Zunino A, Poggi A, Mascelli S, Raso A and Frosina G: Predictability, efficacy and safety of radiosensitization of glioblastoma-initiating cells by the ATM inhibitor KU-60019. Int J Cancer *135*: 479-491, 2014.

37 Biddlestone-Thorpe L, Sajjad M, Rosenberg E, Beckta JM, Valerie NC, Tokarz M, Adams BR, Wagner AF, Khalil A, Gilfor D, Golding SE, Deb S, Temesi DG, Lau A, O'Connor MJ, Choe KS, Parada LF, Lim SK, Mukhopadhyay ND and Valerie K: ATM kinase inhibition preferentially sensitizes p53-mutant glioma to ionizing radiation. Clin Cancer Res *19*: 3189-3200, 2013.

Received April 15, 2016
Revised May 23, 2016
Accepted May 25, 2016